

Solvent effect induced charge polarity switching from p- to n-
type in polyaniline and carbon nanotubes hybrid films with
high thermoelectric power factor

Yizhuo Wang^{1‡}, Xu Dai^{1‡}, Jiahao Pan¹, Jing Wang², Xu Sun¹, Kuncai Li¹,
Hong Wang^{1,2*}

¹ State Key Laboratory of Multiphase Flow in Power Engineering & Frontier
Institute of Science and Technology, Xi'an Jiaotong University, Xi'an, 710054,
China

²School of Energy and Power Engineering, Xi'an Jiaotong University, Xi'an,
710054, China

E-mail: hong.wang@xjtu.edu.cn

[‡]These two authors contribute equally to the paper.

EXPERIMENTAL SECTION

Materials

Single-walled carbon nanotube (SWCNT) was purchased from Nanjing XFNANO Materials Tech. Co. Ltd, China. Polyaniline (PANI-eb) (average $M_w \sim 50000$) was purchased from Sigma-Aldrich Co., Ltd., U.S.A. N-methylpyrrolidinone (NMP) was purchased from Aladdin Co., Ltd., China. Dimethyl sulfoxide (DMSO) was purchased from Energy Chemical Co. Ltd, China.

Preparation of SWCNT only films :

5 mg SWCNT was added to DMSO or distilled water (H_2O), respectively. The mixed solution was sonicated with a pen-type ultrasonic (FS-250N, 105W) for 2 h. After vacuum filtration, the obtained SWCNT films were washed thoroughly with their neat solvents. Finally, the SWCNT films were dried in a vacuum at 60 °C under N_2 protection

Preparation of PANI/SWCNT hybrid films :

Two methods (the sonicating method and the stirring method) were used to prepare PANI/SWCNT hybrid films.

The sonicating method: 5 mg SWCNT and 10 wt.%, 20 wt.%, 30 wt.%, 50 wt.% PANI were added to DMSO or distilled water (H_2O), respectively. The mixed solution was sonicated with a pen-type ultrasonic (FS-250N, 105W) for 2 h. After vacuum filtration, the obtained PANI/SWCNT hybrid films were washed thoroughly with their neat solvents. Finally, the PANI/SWCNT hybrid films were dried at 60 °C under N_2 protection.

The stirring method: 5 mg SWCNT was added to DMSO. The mixed solution was sonicated with a pen-type ultrasonic (FS-250N, 105W) for 2 h. Then, 10 wt.% PANI was added to SWCNT dispersion. The mixture solution was stirred for 2 h. After vacuum filtration, the obtained PANI/SWCNT hybrid films were washed thoroughly with their neat solvents. Finally, the PANI/SWCNT hybrid films were dried at 60 °C under N_2 protection.

Synthesis of PANI-Ib powder :

The PANI-Ib powder was synthesized according to previously reported literature¹. 0.5~1 wt.% PANI-eb powder was added to NMP and heated for 2h at 160~180 °C under nitrogen protection. The solution is then heated in a glove box to remove the NMP solvent.

Preparation of compressed PANI/SWCNT hybrid films :

The PANI/SWCNT hybrid films were cut into strips of 15 mm in length and 4 mm in width. A strip of hybrid films was sandwiched between two pieces of polyethylene terephthalate (PET) films and then placed on a tablet press (YLJ-24T, HEFEI KEJING). A pressure of 2 MPa was applied and held for a certain period of time (2~28 min). Subsequently, the compressed hybrid films were peeled off from the PET films and the stripped films were immersed in DMSO. Finally, the compressed PANI/SWCNT hybrid films were dried at 60 °C under N₂ protection.

After being exposed to air for a certain time, the PANI-eb₁₀/SWCNT hybrid film turned p-type. They would return to n-type by immersing the air-exposed hybrid film in DMSO for 2 h and put in the vacuum oven before and after purging N₂ three times at 60 °C for 2 h.

Measurements

The electrical conductivity and Seebeck coefficient were measured by the JouleYacht MRS-3RT thin film thermoelectric test system. The thermal conductivity was measured by LFA-467, NETZSCH, Germany. The output voltage and output power of the thermoelectric device were measured by Keithley 2400. Scanning electron microscope images were obtained with a field emission scanning electron microscopy, QUANTA FEG 250. The Raman spectra were measured by Laser Raman Spectrometer with an excitation wavelength of 532 nm. Fourier Transform Infrared spectra (FTIR) were recorded within the wavenumber range of 600–4000 cm⁻¹ through Thermo Fisher, Nicolet 6700. UV–vis spectra of PANI samples dissolved in DMSO were recorded as the absorbance measurements at room temperature in the 200–

1000 nm wavelength range using a PE Lambda 950 Spectrophotometer.

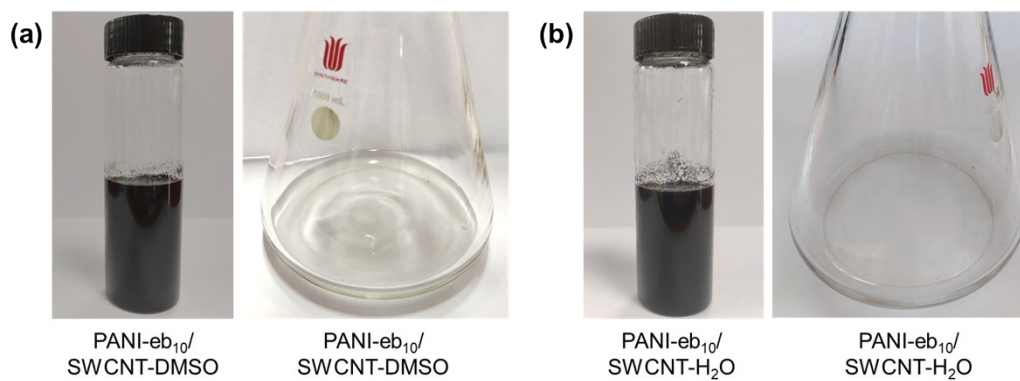


Figure S1, optical images of suspension and the filtrate of PANI-eb₁₀/SWCNT-DMSO (a) and PANI-eb₁₀/SWCNT-H₂O (b).

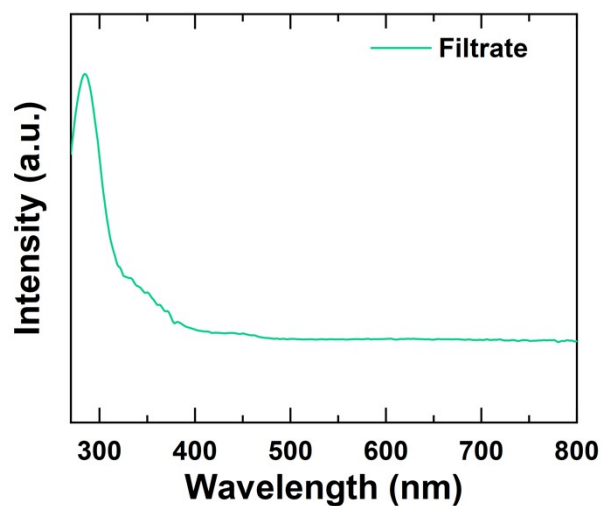


Figure S2, the UV-vis spectrum of filtrated DMSO after the washing process.

For the UV-vis spectrum of filtrate of the PANI-eb₁₀/SWCNT-DMSO, the main peak at 283 nm is supposed to be the benzenoid rings of PANI, revealing little PANI is contained and no SWCNT is observed in the filtrate.

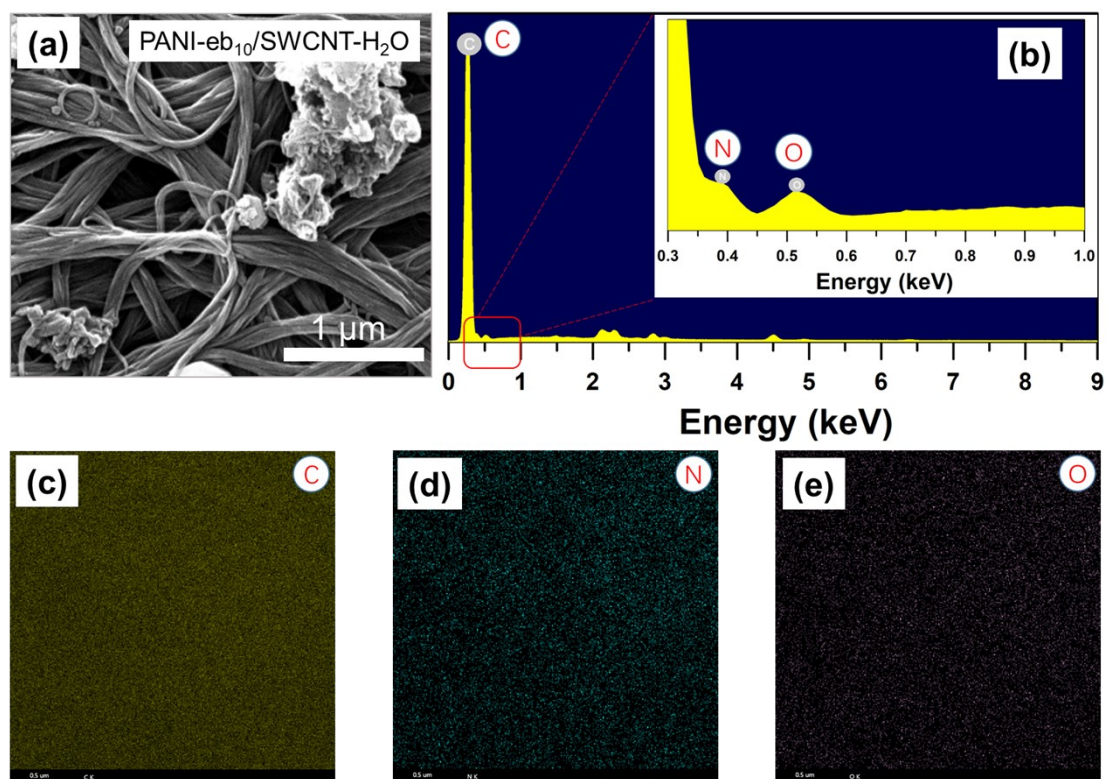


Figure S3, (a) SEM image of PANI-eb₁₀/SWCNT-H₂O films; (b) Energy dispersive spectra (EDS) spectra of the nanoparticles in PANI-eb₁₀/SWCNT-H₂O films; EDS mapping of C (c), N (d) and O (e) for the nanoparticles in PANI-eb₁₀/SWCNT-H₂O films.

EDS spectra show that the nanoparticles contain N, which indicates that they are PANI-eb nanoparticles.

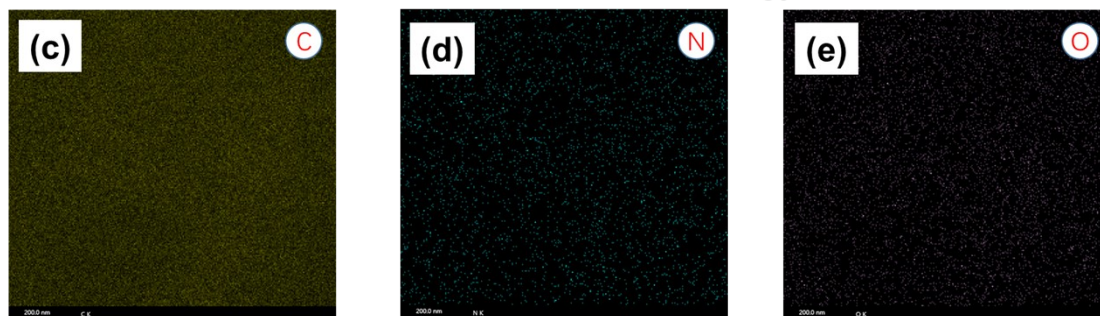
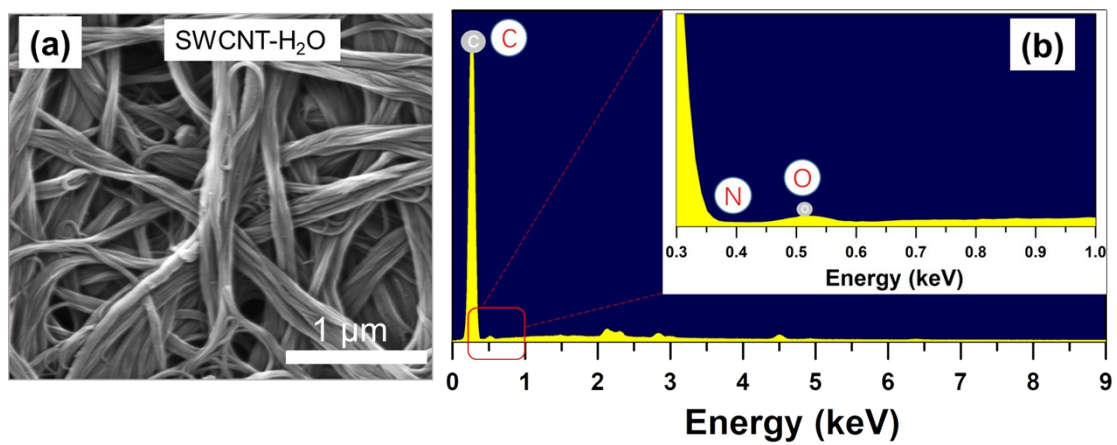


Figure S4, (a) SEM image of SWCNT-H₂O films; (b) EDS spectra of the bundles in SWCNT-H₂O films; EDS mapping of C (c), N (d) and O (e) for the bundles in SWCNT-H₂O films.

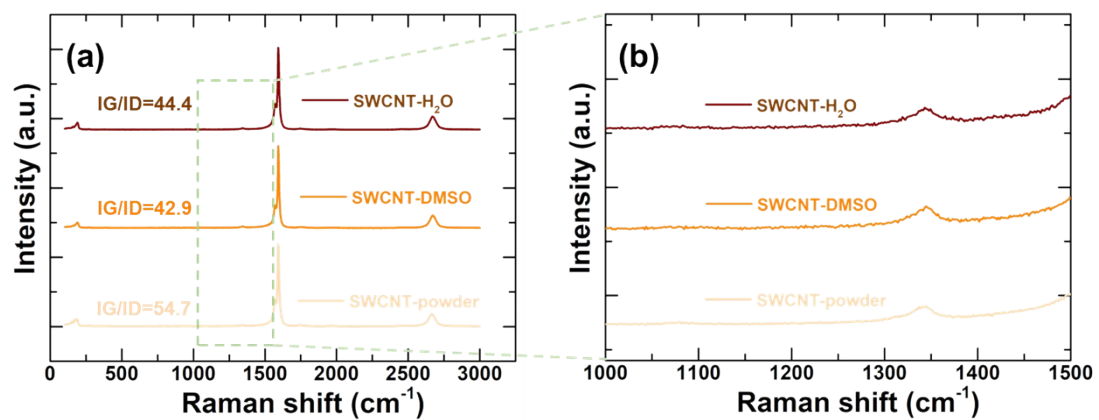


Figure S5, (a) Raman spectra and (b) enlarged Raman spectra for SWCNT-H₂O, SWCNT-DMSO, and original SWCNT powder.

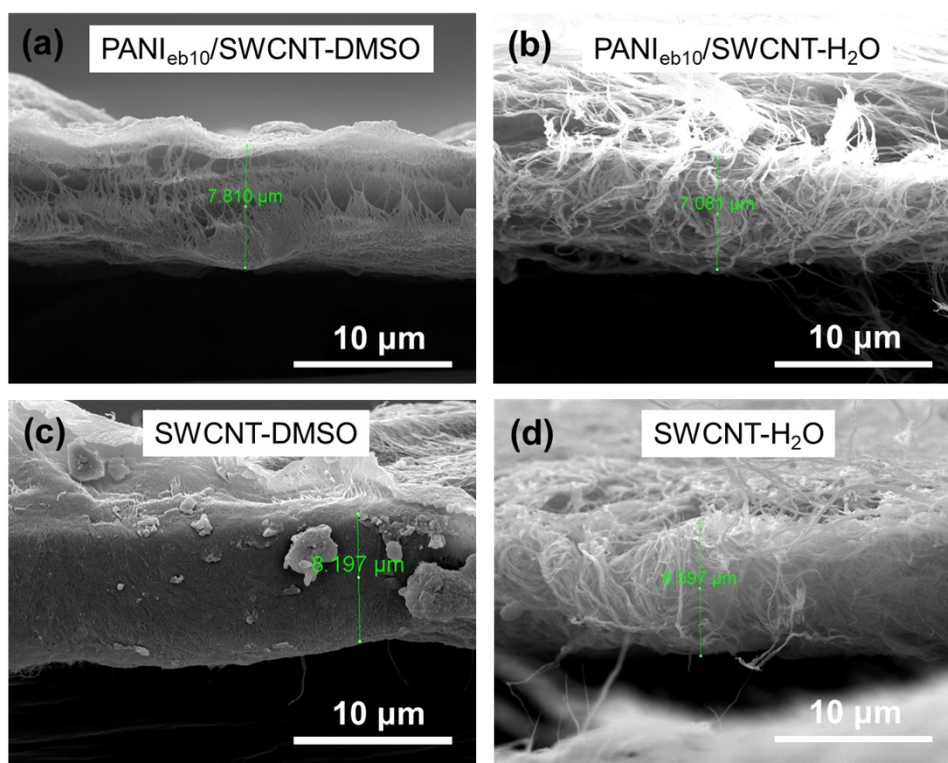


Figure S6, SEM images of the cross-section of PANI-eb₁₀/SWCNT-DMSO (a), PANI-eb₁₀/SWCNT-H₂O (b), SWCNT-DMSO (c) and SWCNT-H₂O films (d).

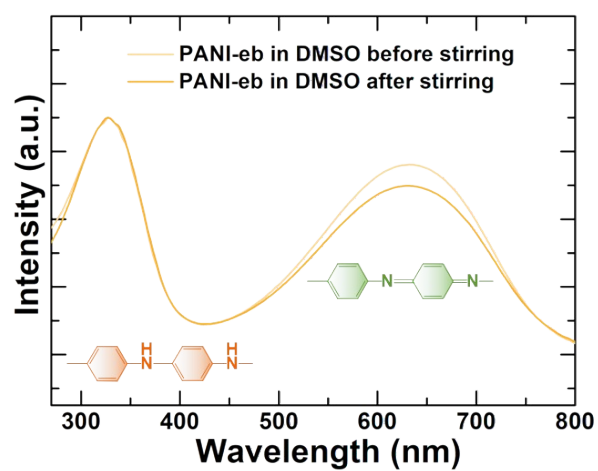


Figure S7, the UV-vis spectra of PANI-eb in DMSO before and after stirring.

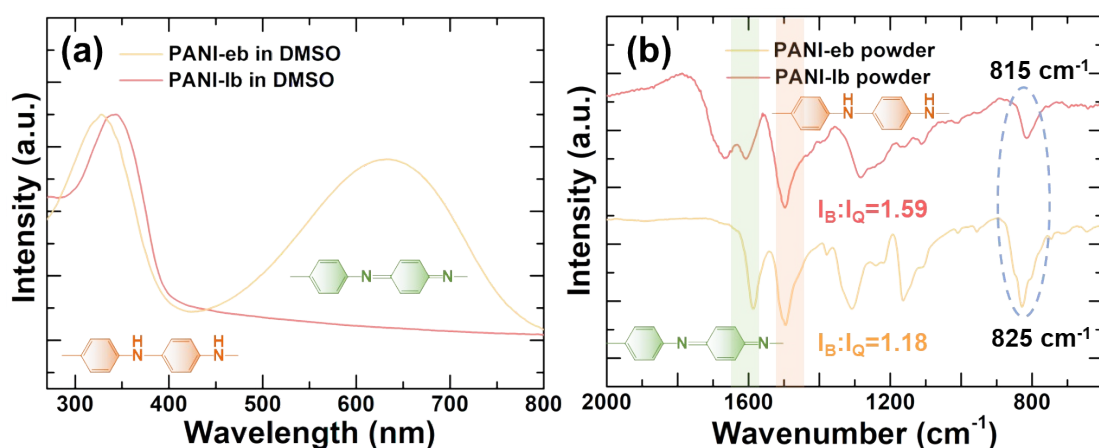


Figure S8, the UV-vis spectra (a) of PANI-eb and PANI-lb in DMSO; the FTIR spectra (b) of PANI-eb and PANI-lb powder.

PANI-lb was synthesized with PANI-eb as the starting material according to literature¹, which was identified by UV-vis and FTIR spectra (**Figure S8**). **Figure S8a** shows that the UV-vis spectra of PANI-eb and PANI-lb in DMSO. There are two peaks appeared at 328 nm and 632 nm for the original PANI-eb solution, which are assigned to the benzenoid rings and the quinoid rings, respectively^{2, 3}. When PANI-eb was heated under N₂ in NMP, the peak for quinoid rings almost disappeared while the peak for benzenoid rings shifted to 343 nm, which is consistent with previous literature reports¹. **Figure S8b** shows that the FTIR spectra of PANI-eb and PANI-lb powder. The absorption peak for 1,4-disubstituted phenyl which appears at 825 cm⁻¹ for emeraldine base, is shifted to 815 cm⁻¹, which is consistent with the FTIR spectra reported for leucoemeraldine base⁴.

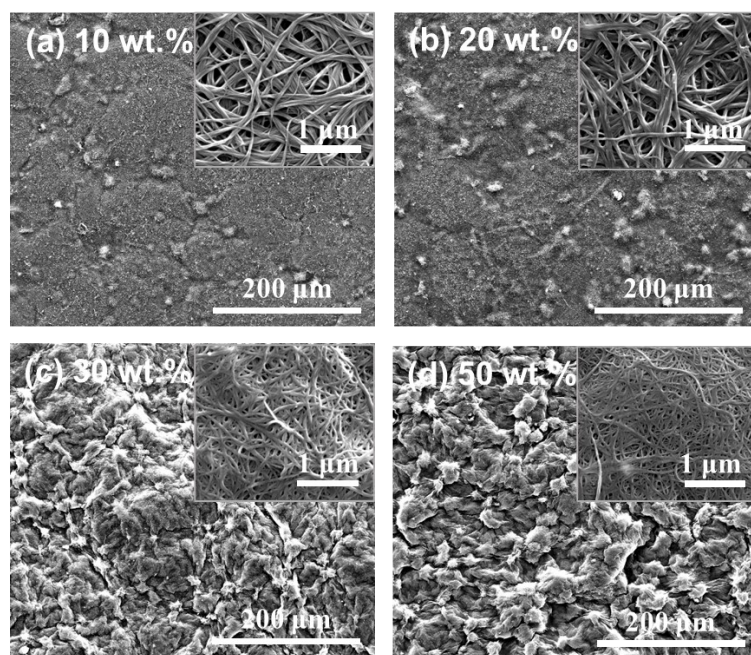


Figure S9, the low and high magnification SEM images of (a) 10 wt.%, (b) 20 wt.%, (c) 30 wt.%, and (d) 50 wt.% PANI-eb/SWCNT hybrid film.

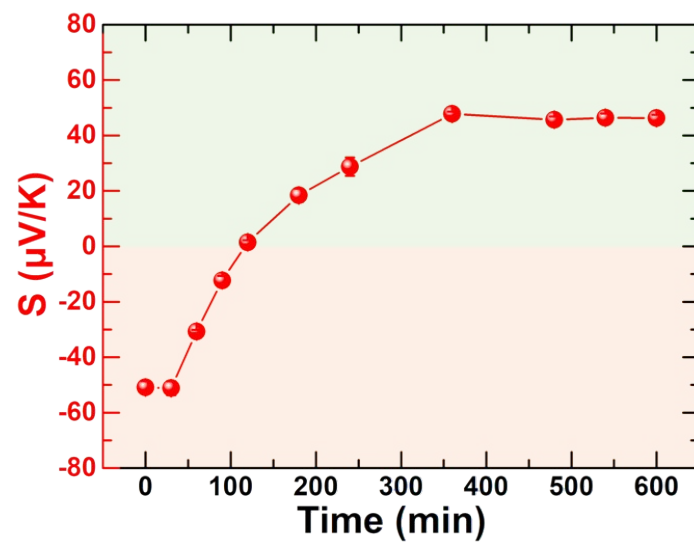


Figure S10, the Seebeck coefficient changing with time while the n-type PANI- eb_{10} /SWCNT-DMSO hybrid film is exposed to the air.

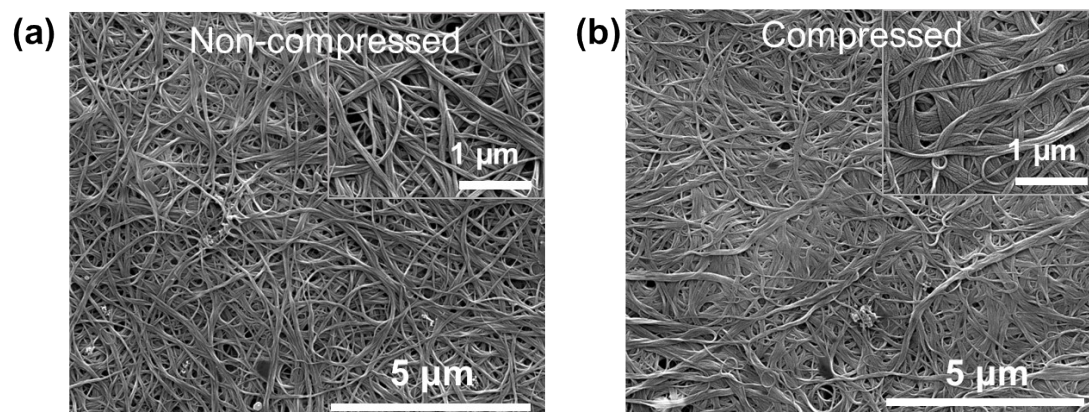


Figure S11, SEM images of PANI-eb₁₀/SWCNT-DMSO hybrid films before (a) and after (b) being compressed for 16 min.

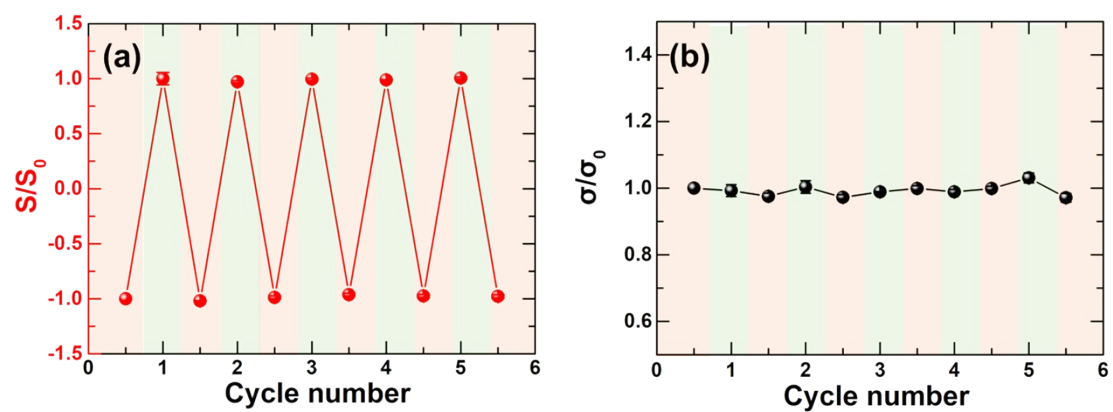


Figure S12, the Seebeck coefficient (a) and the electrical conductivity (b) of compressed PANI-eb₁₀/SWCNT-DMSO hybrid film when exposed to the air and immersed in DMSO.

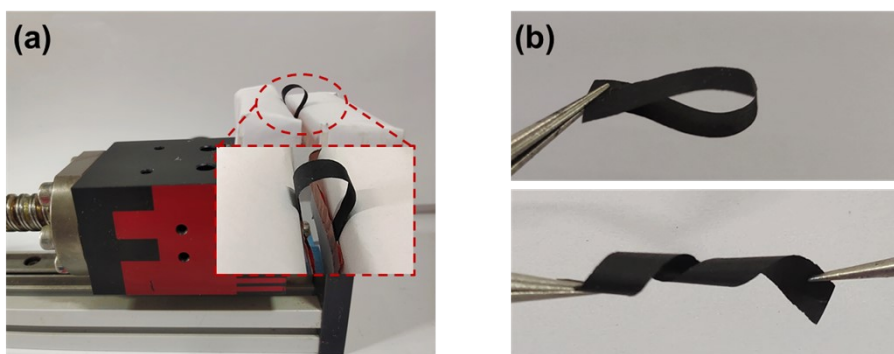


Figure S13, Optical image of the bending instrument (a) and flexible compressed PANI- eb_{10} /SWCNT-DMSO hybrid films

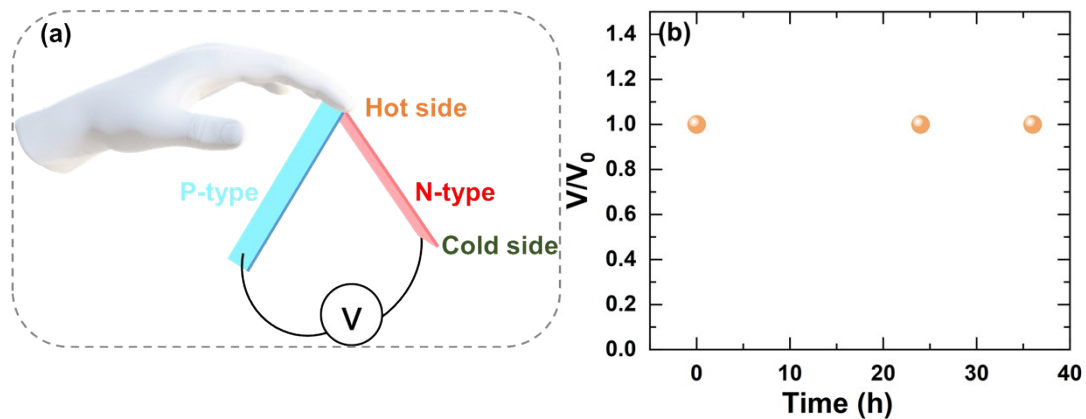


Figure S14, (a) the illustration of the test process of the output voltage, and (b) the normalized output voltage of one pair of p-n modules as a function of time in the glove box.

The output performance of single-piece device stability is evaluated as shown in **Figure S14**. The testing process of the output voltage is shown in **Figure S14a**. The single-piece device is ~ 4 mm in width and ~ 35 mm in length composed of a one-pair p-n module and stored in the glove box. When the human finger and the environment serve as the hot and cold sides for the device, respectively, the output voltage is nearly consistent over 36 h (**Figure S14b**).

Table S1 Comparison of thermoelectric properties for PANI/CNT composites.

Materials	σ , S/cm	S, $\mu\text{V/K}$	PF, $\mu\text{W/m-K}^2$	Ref
Compressed n-type SWCNT/PANI	3980.7	-50.8	1031	This work
Compressed p-type SWCNT/PANI	3951.7	52.3	1079	This work
CNTF/PANI	1452.7	55.5	447.4	5
SWCNT/PANI	2898	33.3	321	6
PANI/SWCNT	842.5	60	236.4	7
SWCNT/PANI-CSA	1440	38.9	217	8
PANI/SWCNT	1895	33.1	207.3	9
SWCNT/PANI-CSA	769	48	176	10
SWCNT/PANI fiber	1856	30.8	176	11
SWCNT/PANI	1965	24.1	114.4	12
PANIPy/SWCNT	418.8	41	70.4	13
HCl-doped PANIeb/SWCNT	29.95	119	42.4	14
SWNT/PANI	12.5	40	20	15
SWCNT/PANI	289	18.9	10.3	16
SWCNT/PANI	31.53	45.4	6.50	17

Table S2 Comparison of thermoelectric properties for PANI/CNT composites.

Sample	σ (S/cm)
PANI-Ib ₁₀ /SWCNT-DMSO hybrid films prepared by the stirring method	775.24±15.16
PANI-Ib ₁₀ /SWCNT-DMSO hybrid films prepared by the sonicating method	724.05±28.31
PANI-eb ₁₀ /SWCNT-DMSO hybrid films prepared by the stirring method	668.12±107.12
PANI-eb ₁₀ /SWCNT-DMSO hybrid films prepared by the sonicating method	1007.8±58.9

References

1. A. Afzali, S. L. Buchwalter, L. P. Buchwalter and G. Hougham, *Polymer*, 1997, **38**, 4439-4443.
2. S. Wang, J. Shang, Q. Wang, W. Zhang, X. Wu, J. Chen, W. Zhang, S. Qiu, Y. Wang and X. Wang, *ACS Appl. Mater. Interfaces*, 2017, **9**, 43939-43949.
3. C. A. Amarnath, J. Kim, K. Kim, J. Choi and D. Sohn, *Polymer*, 2008, **49**, 432-437.
4. Y. Furukawa, F. Ueda, Y. Hyodo, I. Harada, T. Nakajima and T. Kawagoe, *Macromolecules*, 1988, **21**, 1297-1305.
5. J. Huang, X. Liu and Y. Du, *J. Materiomics*, 2024, **10**, 173-178.
6. H. Li, Y. Liang, Y. Liu, S. Liu, P. Li and C. He, *Compos. Sci. Technol.*, 2021, **210**, 108797.
7. S. Yin, W. Lu, X. Wu, Q. Luo, E. Wang and C.-Y. Guo, *ACS Appl. Mater. Interfaces*, 2021, **13**, 3930-3936.
8. L. Wang, Q. Yao, J. Xiao, K. Zeng, S. Qu, W. Shi, Q. Wang and L. Chen, *Chem. Asian J.*, 2016, **11**, 1804-1810.
9. P. Yu, R. Wu, C. Liu, J. Lan, Y. Lin and X. Yang, *Sustain. Energy Fuels*, 2023, **7**, 172-180.
10. Q. Yao, Q. Wang, L. Wang and L. Chen, *Energy Environ. Sci.*, 2014, **7**, 3801-3807.
11. H. Li, Y. Liu, S. Liu, P. Li, C. Zhang and C. He, *Compos. Part A Appl. Sci. Manuf.*, 2023, **166**, 107386.
12. L. Feng, R. Wu, C. Liu, J. Lan, Y.-H. Lin and X. Yang, *ACS Appl. Energy Mater.*, 2021, **4**, 4081-4089.
13. S. Wang, F. Liu, C. Gao, T. Wan, L. Wang, L. Wang and L. Wang, *Chem. Eng. J.*, 2019, **370**, 322-329.
14. H. Wang, S.-i. Yi and C. Yu, *Polymer*, 2016, **97**, 487-495.
15. Q. Yao, L. Chen, W. Zhang, S. Liufu and X. Chen, *ACS Nano*, 2010, **4**, 2445-2451.
16. L. Wang, Q. Yao, S. Qu, W. Shi and L. Chen, *Org. Electron.*, 2016, **39**, 146-152.
17. J. Liu, J. Sun and L. Gao, *Nanoscale*, 2011, **3**, 3616-3619.